Ultrasonic and Eddy Current Testing of Nuclear Graphite

Tatsuo IYOKU, Shusaku SHIOZAWA, Norikazu OOKA
Japan Atomic Energy Research Institute, Oarai, Japan
Mamoru KAMBE
Fuji Electric Co., Ltd., Kawasaki, Japan
Akira IDE
Fuji Electric Co., Ltd., Tokyo, Japan

ABSTRACT

Nondestructive testing (NDT) methods of a graphite material for core and core support components were investigated to guarantee the structural integrity of High Tempreture Engineering Test Reactor (HTTR). Ultrasonic testing for detection of internal flaws and eddy current testing for detection of surface flaws were examined in the present study. Fundamental characteristics of flaw detectability were obtained through the investigation and it was confirmed that these testings are effective methods as NDT of a graphite material.

1 INTRODUCTION

NDTs are generally applied to important structural components such as primary pressure boundary for nuclear reactor. Among various NDTs, both ultrasonic and eddy current testings are deemed to be the most promising method as a proof testing of nuclear grade graphite. To clarify the minimum detectable flaw size and establish applicability of the testing method, extensive tests were carried out. The graphite grade used for the test were IG-11 and PGX, which will be employed as the materials of the core and core support components of the HTTR.

2 GRAPHITE MATERIALS AND APPLICATION OF NONDESTRUCTIVE TESTINGS

IG-11 is a fine grain graphite with a mean grain size of 20 μm, while PGX is a middle grain graphite with a maximum grain size of 0.8 mm. The ultrasonic testing is generally suited to detect the internal flaws and is hoped to be applicable to a volumetric testing of the stocks before machining. On the other hand, the eddy current testing is generally used to detect surface flaws, and is scheduled to be applied to a surface testing of the machined stocks.

3 ULTRASONIC TESTING

3.1 Testing method and condition

As the result of a preliminary test, single probe reflection method using 0.5MHz frequency (probe dia.34mm) was found most suitable to apply to IG- 11.
To PGX, both single probe reflection method and double probe reflection method using 0.2MHz frequency (probe dia.28mm) were applied. Water was used as the couplant. Both axial and radial testings were made for the graphite test blocks.

3.2 Test blocks with artificial flaws

Test blocks with artificial flaws were prepared in the tests. The artificial holes with flat bottom hole so that the effective distance of the sound axis were varied from 150-550mm for IG-11 and 130-950mm for PGX, respectively. The diameters of the holes are in the range 5.2-10.4mm for IG-11 and 20-70mm for PGX.

3.3 Sound pressure from the bottom and the circular flaw using circular transducer

(1) Sound pressure along the sound axis

The well-known law of sound pressure along the sound axis is expressed by the equation①, where the attenuation loss can be neglected. Sound pressure at the position of flaw or the bottom is obtained by equation①.

$$\frac{P_B}{P_0} = 2\sin\left(\frac{ka}{2}\cdot\left(1+\left(\frac{X_B}{a}\right)^2\right)^{1/2} - \frac{X_B}{a}\right) \qquad \text{-------} ①$$

where $k = 2\pi/\lambda$, P_0 is average sound pressure immediately in front of the transducer, P_B is sound pressure at distance X_B, X_B is distance along the sound axis, λ is wave length, a is radius of the transducer.

Equation ① may be approximated by the equation② if X_B is more than 3a.

$$\frac{P_B}{P_0} \fallingdotseq 2\sin\frac{k a^2}{4 X_B} = 2\sin\frac{A}{2\lambda X_B} \qquad \text{----------②}$$

where A is area of the transducer.

Then, the sound pressure is modified by the equation③ in case the attenuation is considered.

$$\left(\frac{P_B}{P_0}\right)_{att} \fallingdotseq 2\sin\frac{A}{2\lambda X_B}\cdot e^{-\alpha X_B} \qquad \text{---------- ③}$$

where α is attenuation coefficient.

(2)Sound pressure from circular flaw

The sound pressure from circular flaw on the sound axis at distance X_D is given as equation ④, when the attenuation is considered.

$$\left(\frac{P_D}{P_0}\right)_{att} \fallingdotseq 4\sin\frac{A}{2\lambda X_D}\cdot\sin\frac{S}{2\lambda X_D}\cdot e^{-\alpha X_D} \qquad \text{--------- ④}$$

where P_D is sound pressure from circular flaw at distance X_D, X_D is distance between the transducer and the flaw and S is area of the flaw.

3.4 Test results and discussion

(1) Determination of flaw position

It was observed that the measured flaw positions deviated from the real flaw position. The typical measurement results of flaw position in diametral section for axial testing are shown in Fig.1 (a). Maximum measurement deviations, in case of flaw distance of 400mm, are 35mm for IG-11 and 30mm for PGX. The mesurement results of axial flaw distance are also shown in Fig.1 (b). The Maximum deviation, in case of flaw distance of 400mm, are 8mm (2%) for IG-11 and 15mm (4%) for PGX.

As the cause of the deviation of flaw position, it is supposed that the ultrasonic velocity is not constant and the ultrasonic beam propagates selectively along the most preferred path in the graphite material becouse of large grain size and the irregular density of graphite material.

(2) Determination of detectable flaw size

The minimum detectable flaw size is affected by the degree of attenuation and noise. Typical experimental results of noise echo, flaw echo and bottom echo heights for the axial testing are shown in Fig.2 (a) and (c).

For noise echo, both minimum (Nmin) and maximum height (Nmax) were measured.

The detectable flaw is the flaw with the echo height exceeding the height of noise echo.

The echo heights from diametrers of 5mm and 10mm artificial flaws, as shown in Fig. 2 (a), decrease linearly in the range of the testing distance up to 400 mm. However, the flaw echo heights at testing distance of 600mm decrease non-linearly. As the cause, it is supposed that the ultrasonic attenuation is large at this distance. The flaw echo heights in Fig. 2 (b) and (d) show the heights after the attenuation compensation were performed.

The attenuation is presented in Fig. 2 (a) and (c) as the difference between Bmax and B'max. Bmax is maximum bottom echo height obtained from the test block and B'max is maximum bottom echo height obtained from the adjacent part of artificial flaw. The flaw echo heights were corrected by the value equal to Bmax-B'max. Then, a linear relation was obtained between the distance and the echo height.

The adequacy of Fig. 2 (b) and (d) was investgated theoretically. The theoretical results (equation③ and④) are given by solid lines in the Fig. 2 (b) and (d). Theoretical and experimental results show good agreement in case of IG-11 using 0.5MHz frequency, but in case of PGX using 0.2MHz frequency, agreement is not so good because of large variation of attenuation caused by large grain size (0.8mm).

The typical minimum detectable flaw sizes which were obtained in consideration of the noise echo and the attenuation are shown in Fig. 3 for axial testing of IG-11 and PGX.

In this chart, it is assumed that the flaw of which echo height is more than 4 times of noise echo height (4N) is detectable. Therefore, both the minimum (4Nmin) and the maximum level of 4N (4Nmax) are shown by the region Ⅱ in Fig. 3. Furthermore, minimum detectable flaw size is also changed by attenuation. The regions of fluctuation of attenuation are shown by the area region Ⅰ in Fig. 3. This regions are obtained from the difference between Bmax and B'max. The minimum detectable flaw sizes are practically obtained from the region Ⅰand Ⅱ. The typical minimum detectable flaw sizes are also shown in Table 1.

Table 1. Minimum size of detectable internal circular flaw (Ultrasonic testing) (mm)

Graphite material	Test frequency (Testing method)	Testing direction	Distance 200	400	600
IG-11	0.5 MHz (Single probe)	Axial	2 ～ 4	2 ～ 5	2 ～ 5
		Radial	2 ～ 4	2 ～ 5	—
PGX	0.2 MHz (Single probe)	Axial	12 ～ 13	17 ～ 44	20 ～ 57
		Radial	20 ～ 36	23 ～ 45	25 ～ 55
	0.2 MHz (Double probe)	Axial	12 ～ 24	18 ～ 41	23 ～ 55
		Radial	14 ～ 27	18 ～ 38	20 ～ 43

4 EDDY CURRENT TESTING

4.1 Testing condition and method

As probe, self-induction type coil arrangement with 2 ×1mm ferite was used. This probe was used as differential type. Test frequency was 1MHz. Lift-off was approx. 0.1mm. The probe was moved for scanning at the speed of 100mm/s.

4.2 Test block with artificial flaws

To confirm the test condition and flaw detectability, test blocks with artificial slit flaws and with actual products geometries were prepared in this tests. The sizes of artificial slit flaws are 0.5～ 5mm in length. The artificial slit flaws were scratched on the through hole, on the corner of bottomed hole and on spherical surface of IG-11 made test blocks and on the key way of PGX made test

blocks.

4.3 Test results and consideration

(1) Scanning angle of probe and the effective testing area.
The flaw signal amplitudes are changed by the scanning angle of probe (the angle which is determined by flaw direction and ferite partition direction). The effects of scanning angle of probe were investigated and shown in Fig.4. The area which has 70% signal amplitude is within approximate 1.5mm radius area for both IG-11 and PGX. So probe scanning pitch should be decided equal to or smaller than this effctive radius.

(2) The minimum detectable flaw size
The typical flaw signals are shown in Fig.5. In this test, it is defined that the flaw whose amplitude is more than 3 times of noise amplitude is the detectable flaw. The minimum detectable surface falw size is shown in Table 2.

Table 2. Minimum size of detectable surface slit flaw (Eddy current testing) (mm)

Graphite material	Part of detection	Flaw direction	Probe scanning angle	Depth 0.5	Depth 1.0
IG-11	Through hole for	Axial	0°	2.0	2.0
			45°	—	2.0
	Nuclear fuel	Tangencial	0°	2.0	2.0
			45°	2.0	2.0
	Hole with bottom	Axial	0°	×	1.0
	(corner)	Tangencial	0°	×	1.0
	Spherical surface	Radial	0°	1.0	1.0
			45°	2.0	1.0
PGX	Key way	Axial	0°	—	—
			45°	—	—
		Tangencial	0°	—	5.0
			45°	—	—
	Key way end	Axial	0°	×	5.0
		Radial	0°	×	3.0

— : not detected × : not preparated

5 CONCLUSIONS

To clear and establish applicability and the minimum detectable flaw size of ultrasonic and eddy current testings for graphite materials of the HTTR, extensive tests were carried out.
By this test, it was confiremed that these testings are effective methods as NDT of graphite materials.
The detectable flaw sizes by these NDT do not necessarily gurantee the design requirements. Howevore, these methods still seem to be the most sensible and practical among available other NDTs at present. Thus, these two NDTs should be recommended to be used as the proof testing for HTTR graphite materials.

REFERENCE

(1) The Japanese society for nondestractive inspection. 1989. Ultrasonic Testing Ⅲ. Tokyo Japan.

(3) IDE A., KAMBE M. 1990. Eddy current testing for graphite materials. FAPIG No.124 : pp35 ～ 39.

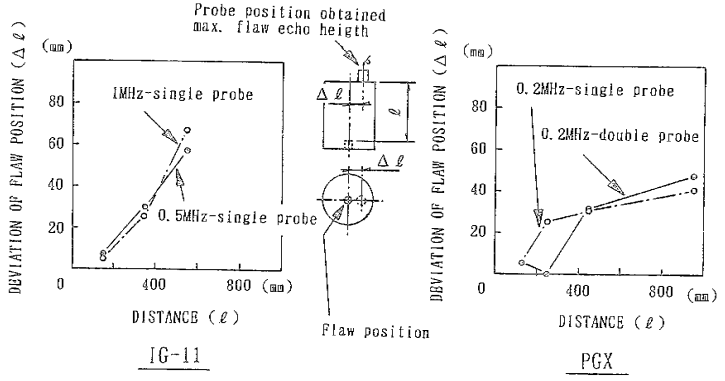

(a) Flaw position in diametral section

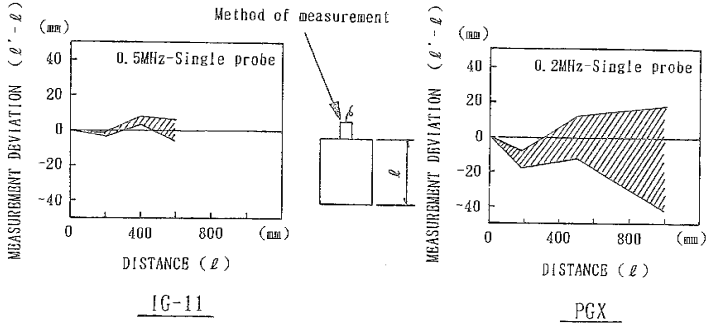

(b) Flaw distance

Fig. 1. Measurement results of flaw position (Axial testing)

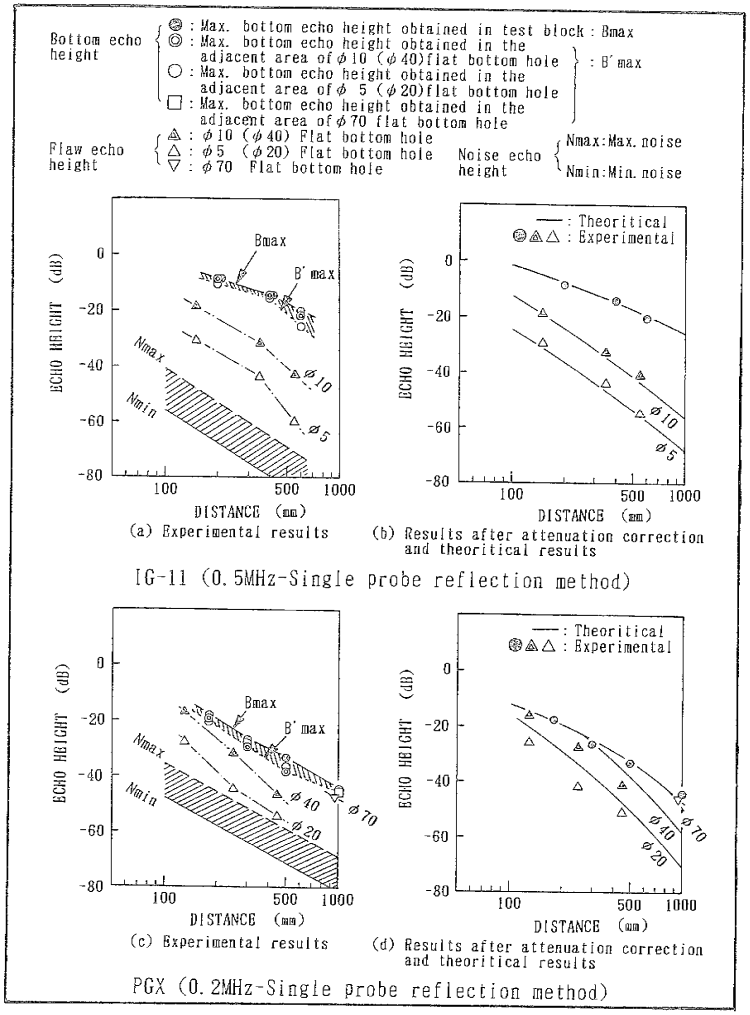

Fig. 2. Distance-amplitude and attenuation characteristic of noise echo and flaw echo height (Axial testing)

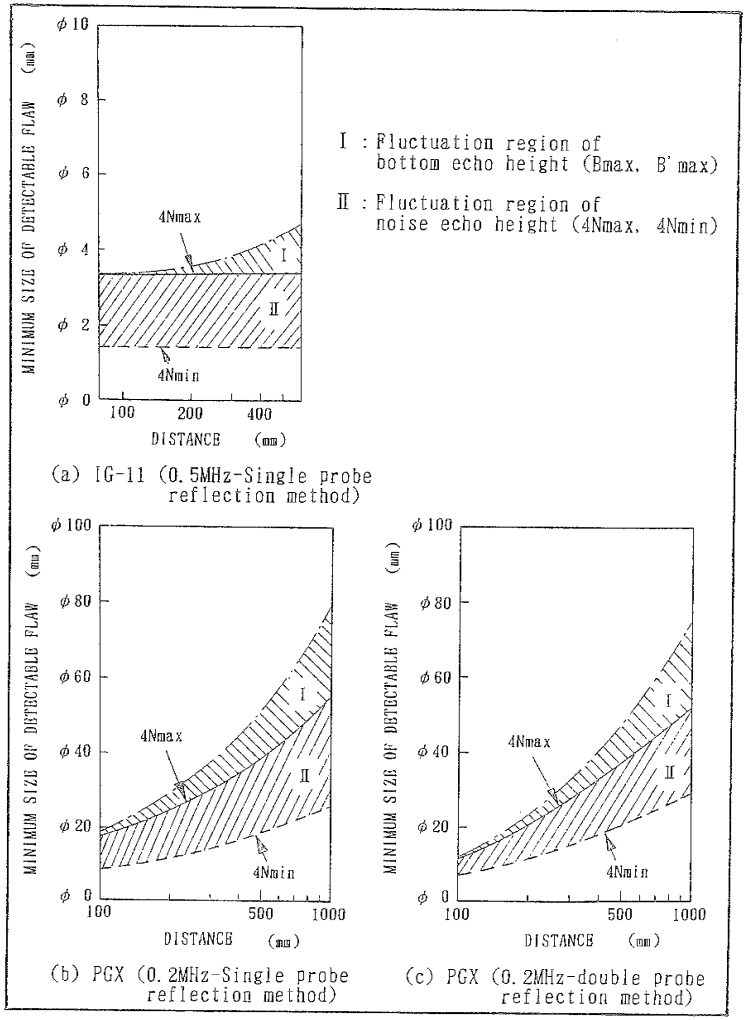

Fig. 3. Minimum size of detectable flaw (Axial testing)

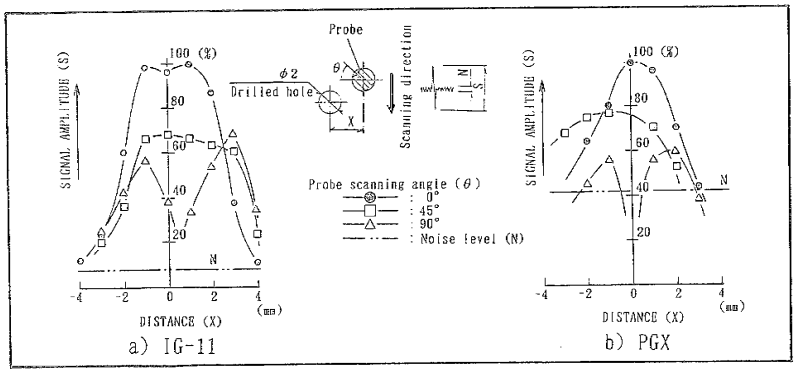

Fig. 4. Signal amplitude for probe scanning angle

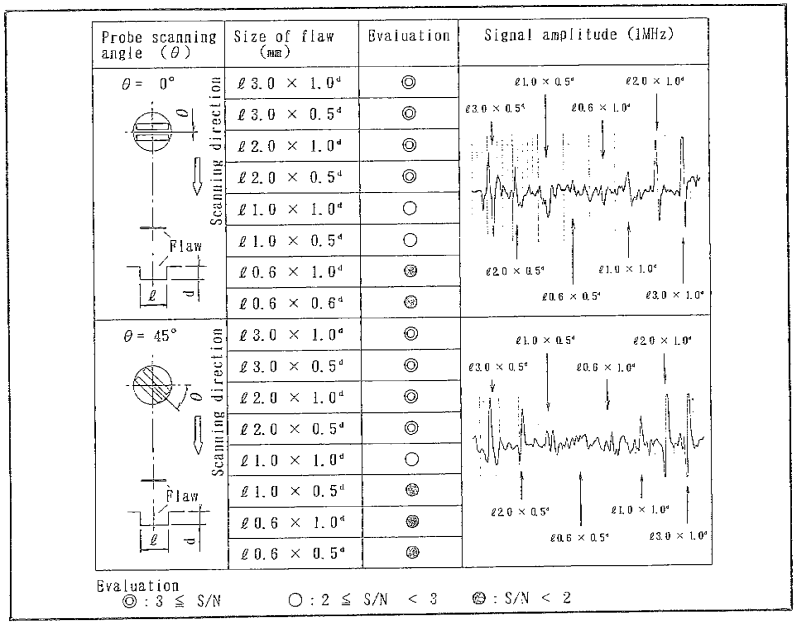

Fig. 5. Typical measurement results of surface flaw for IG-11 (Tangential flaw on the inner surface of through hole, axial testing)